A R C H I V E S O F M E T A L L U R G Y A N D M A T E R I A L S
Volume 60 2015 Issue 4
DOI: 10.1515/amm-2015-0405

A. CZARSKI*,#, T. SKOWRONEK*, P. MATUSIEWICZ*

STABILITY OF A LAMELLAR STRUCTURE – EFFECT OF THE TRUE INTERLAMELLAR SPACING ON THE DURABILITY OF A PEARLITE COLONY

STABILNOŚĆ STRUKTURY PŁYTKOWEJ – WPŁYW RZECZYWISTEJ ODLEGŁOŚCI MIĘDZYPŁYTKOWEJ NA TRWAŁOŚĆ KOLONII PERLITU

A lamellar microstructure is, beside a granular and dispersive one, the most frequently observed microstructure in the case of metal alloys. The most well-known lamellar microstructure is pearlite, a product of a eutectoidal transformation in the Fe-Fe_3C system. The lamellar morphology of pearlite – cementite and ferrite lamellae placed interchangeably within one structural unit described as a colony – is dominant. The durability of the lamellar morphology is much diversified: in the microstructure of spheroidizingly annealed samples, one can observe areas in which the cementite is thoroughly spheroidized, next to very well-preserved cementite lamellae or even whole colonies of lamellar pearlite. The mentioned situation is observed even after long annealing times. The causes of such behaviour can vary. The subject of the previous work of the authors was the effect of the orientation between the ferrite and the cementite on the stability of the lamellar morphology. This work constitutes a continuation of the mentioned paper and it concerns the effect of the true interlamellar spacing on the stability of the lamellar morphology of cementite.

Keywords: true interllamelar spacing, lamellar microstructure, pearlite spheroidization

Mikrostruktura płytkowa to obok ziarnistej i dyspersyjnej jedna z najczęściej spotykanych w przypadku stopów metali. Najbardziej znaną mikrostrukturą płytkową jest perlit, produkt przemiany eutektoidalnej w układzie Fe-Fe_3C. Morfologia płytkowa perlitu –płytki ferrytu i cementytu ułożone na przemian w obrębie jednej jednostki strukturalnej określanej mianem kolonii - jest dominująca. Trwałość morfologii płytkowej jest bardzo zróżnicowana - w mikrostrukturze próbek wyżarzanych sferoidyzująco obserwuje się obszary, w których cementyt jest zupełnie zesferoidyzowany obok bardzo dobrze zachowanych płytek cementytu lub wręcz całych kolonii perlitu płytkowego. Opisana sytuacja ma miejsce nawet po długich czasach wyżarzania. Przyczyny takiego zachowania mogą być różne. Przedmiotem wcześniejszej pracy autorów był wpływ orientacji pomiędzy ferrytem a cementytem na stabilność morfologii płytkowej. Niniejszy artykuł stanowi kontynuację pracy wspomnianej wcześniej i dotyczy wpływu rzeczywistej odległości międzypłytkowej na stabilność morfologii płytkowej cementytu.

1. Introduction

The spheroidization process of pearlite consists in a change in the shape of the cementite lamellae into a spherical one, with the preservation of the constancy of the phase volume, this being possibly accompanied by diffuse growth [1-3].

The complexity of the processes taking place during the spheroidization has its source both in the substructure of ferrite and cementite and the geometrical characteristics of the phases (diversions from the lamellar morphology) as well as the properties of the interfaces etc. The course of the spheroidization process of cementite is non-homogeneous; in the microstructure of the spheroidizingly annealed samples, one can observe areas in which the cementite is fully spheroidized, next to very well-preserved cementite lamellae or even whole colonies of lamellar pearlite. This situation occurs even after long annealing times. The causes of such behaviour are unknown. One of the potential reasons may be the differences in the true interlamellar spacing.

The aim of the performed research was to determine the distribution of the true interlamellar spacing for the colony of lamellar cementite remaining in the microstructure, after different times of spheroidizing annealing. The basis for the determination of the discontinuous (discrete) distribution of the true interlamellar spacing were empirical distributions of the apparent interlamellar spacing. Mechanical properties of the alloys with lamellar microstructure are heavily dependent on the true interlamellar spacing [4, 5].

* AGH UNIVERSITY OF SCIENCE AND TECHNOLOGY, DEPARTMENT OF PHYSICAL AND POWDER METALLURGY, FACULTY OF METALS ENGINEERING AND INDUSTRIAL COMPUTER SCIENCE, AL. MICKIEWICZA 30, 30-059 KRAKÓW, POLAND

Corresponding author: czarski@agh.edu.pl

2. Mechanism and kinetics of perlite spheroidization

For the analysis of pearlite spheroidization mechanism one can distinguish several partial structural processes: fragmentation, rounding off small plate segments into spherical particles, particle coarsening, growth of ferrite grains.

There are many conceptions regarding a mechanism of spheroidization process: the Raylegh's perturbation theory [6-9], the thermal groove theory [10-13], the fault migration theory [6]. Unfortunately, the conceptions mentioned above do not explain fully the mechanism of spheroidization process, but in the area of possible interpretations they rather complete each other. Besides, none of the mentioned conceptions consider satisfactorily the factors like e.g. anisotropy of energy of interphase boundary ferrite/cementite etc.

The results of investigations of pearlite spheroidization kinetics do not also lead to unique conclusions. Values of process activation energy mentioned in a literature are characterized by a large discrepancy – from 90 kJ/mol [14], up to 290 kJ/mol [15]. An activation energy in range of 123÷147 kJ/mol was found for the spheroidization process by Skowronek and Czarski [16]. This range of values shows good agreement with the activation energy for iron and carbon diffusion along a ferrite/cementite interface, so a coupled interface diffusion is the rate-controlling process.

3. Lamellar microstructure

3.1. Selected stereological relations

The quantitative parameters characterizing the lamellar microstructure, i.e. the true (l_t), apparent (l_a) and random (l_r) interlamellar spacing, were defined by DeHoff, Rhines [17] and Underwood [18].

Czarski et al. [19-21] presented a set of stereological relations for the lamellar microstructure, discussed as a model – a packet of parallel planes. The true spacing between the neighbouring planes, i.e. l_t, is a random variable, which is fully described by the function of density $f(l_t)$.

Based on the defined geometrical model of the lamellar microstructure, the conditional function of density of the apparent interlamellar spacing $f(l_a|l_t)$ assumes the form [22, 23]:

$$f(l_a|l_t) = \frac{{l_t}^2}{{l_a}^2\sqrt{{l_a}^2-{l_t}^2}} \;\; ; \;\; l_t \leq l_a < \infty \qquad (1)$$

One can obtain the functions of density of the apparent interlamellar spacing $f(l_a)$) by solving the integral equations:

$$f(l_a) = \int_0^{l_a} f(l_a|l_t) f(l_t) dl_t \qquad (2)$$

3.2. Estimation of true interlamellar spacing distribution in discrete form

Solving equation (2) allows us to determine the distribution of the true interlamellar spacing on the basis of the distribution of the apparent interlamellar spacing. Equation (2) can be treated as the Volterra equation of the first kind with a kernel $f(l_a|l_t)$ for the given function $f(l_a)$ and the unknown function $f(l_t)$. For the given kernel $f(l_a|l_t)$, equation (2) can be solved either analytically or numerically (by approximation).

Let us assume that the function $f(l_a)$ is represented discretely (for m classes, width Δ, in points $l_{ai}=(i-0{,}5)\Delta$, $i=1,....,k$ by probability function $P(l_{ai})$; $P(l_{ai})=\int f(l_a)dl_a$ in range from $l_{ai}-\Delta/2$ to $l_{ai}+\Delta/2$). The function $f(l_t)$ will be represented discretely (for m classes, width Δ, in points $l_{ti}=i\Delta$, $i=1,...,k$ by probability function $P(l_{ti})$; $P(l_{ti})= \int f(l_t)dl_t$ in range from $l_{ti}-\Delta/2$ to $l_{ti}+\Delta/2$.

For calculational reasons, it will be comfortable to apply the relative interlamellar spacings, i.e. l_a/l_{amin} and l_t/l_{tmin}, where: l_{amin} is the lowest measured value of the apparent interlamellar spacing l_a, and l_{tmin} is the minimal value of the true interlamellar spacing l_t (with assumption: $l_{amin}= l_{tmin}$).

If the values of the discrete functions $P(l_{ai}/l_{amin})$ and $P(l_{ti}/l_{tmin})$ are treated as components of vectors **P** and **T**, respectively, then, for the given vector **P**, the approximated solution of equation (2), for the unknown vector **T**, has the following form:

$$\mathbf{T}=\mathbf{W}^{-1}\mathbf{P} \qquad (3)$$

where: $\mathbf{W}^{-1}$ – is the inverse matrix for the matrix **W** described by the kernel of equation (2).

A complete description of the solution method for equation (2) in the discrete form, as well as the matrices **W** and $\mathbf{W}^{-1}$ of the assumed values of Δ, and m, are included in the work of Czarski and Ryś [24].

4. Experimental

The aim of the performed research was to determine the distribution of the true interlamellar spacing for the colony of lamellar cementite remaining in the microstructure, after different times of spheroidization annealing. The basis for the determination of the discontinuous (discrete) distribution of the interlamellar spacing were the empirical distributions of the apparent interlamellar spacing.

The investigated material was a Fe-C model alloy with the carbon content of 0.76% (mass.).

- In order to obtain the structure of thick-lamellar pearlite, thermal treatment was performed, consisting in austenitization of the samples in a furnace with a salt bath (50% $BaCl_2$ + 50% NaCl) of the temperature of 900°C during 0.5 hour, followed by the samples being quickly transferred to a furnace with a lead bath of the temperature of 700°C, where a pearlite transformation took place under isothermal conditions. The time of the isothermal annealing (3.5 hours) was determined experimentally.
- The spheroidizing (isothermal) annealing was performed at the temperature of 700ºC, for the following times: 5, 50, 100, 400 hours. The treatment was performed in a sylite chamber furnace with thyristor temperature control. The accuracy of the temperature maintenance was ±2°C.

The microscopic observations of the microstructure, both in the initial state and after the spheroidizing annealing, were

conducted by means of the light microscope NU2-Zeiss. The microstructure was revealed with a 2% solution of picric acid in ethyl alcohol (picral). Selected microstructures are presented in Fig. 1.

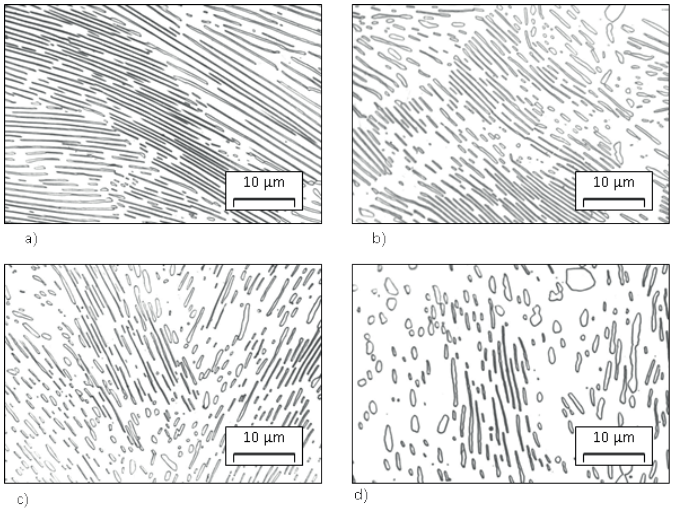

Fig. 1. Pearlite microstructure isothermally annealed at a 700ºC during: a) the initial state, b) 50, c) 100, and d) 400 hours (etched in picral).

5. Measurement methodology, test results

In reference to both the initial microstructure (thick-lamellar pearlite) and the microstructures after the spheroidizing annealing, the apparent interlamellar spacing was measured l_a. A schematic of a single measurement of the apparent interlamellar spacing l_a is presented in Fig. 2. Estimation of l_a and l_r with computer image analysis methods is presented in [25].

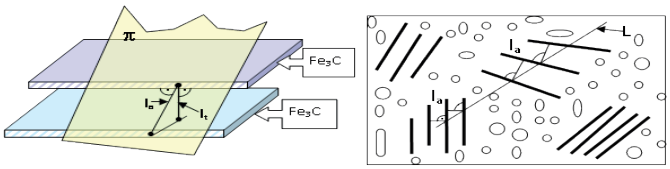

Fig. 2. Quantitative parameters of a lamellar microstructure, diagram of measuring of the apparent interllamelar spacing.

In order to perform the measurement, a random secant L was plotted on the microstructure image. From the intersection point of the secant with the cementite lamella, a normal was drawn: the length of the interval connecting the centers of the neighbouring lamellae constitutes the measured apparent interlamellar spacing l_a. The measurements were performed on microstructure images with the total resolution of 2500×. The accuracy of a single measurement of the spacing l_a equaled 0.2×10^{-3} mm. The measurement results are presented in Table 1.

On the basis of the distributions of the apparent interlamellar spacing (Table 1) it was possible to determine – according to the presented approximation method (expression (3)) – the discrete distributions of the true interlamellar spacing l_t. The results are show in Table 2 and Fig. 3.

TABLE 1

Empirical distributions of the apparent interllamelar spacing in remaining fraction of microstructure of lamellar cementite

Class number	$l_{ai}\cdot10^3$, mm	$l_{ai}/l_{a\,min}$	The initial state		5 hours		50 hours		100 hours		400 hours	
			n_i	n_i/n	n_i	n_i/n	n_i	n_i/n	n_i	n_i/n	n_i	n_i/n
1	0.4÷0.6	1.0÷1.5	197	0.1833	102	0.1220	48	0.1011	17	0.0497	14	0.0465
2	0.6÷0.8	1.5÷2.0	520	0.4837	350	0.4187	139	0.2926	87	0.2544	58	0.1927
3	0.8÷1.0	2.0÷2.5	228	0.2121	221	0.2644	144	0.3032	94	0.2749	80	0.2658
4	1.0÷1.2	2.5÷3.0	79	0.0735	91	0.1089	73	0.1537	65	0.1901	70	0.2325
5	1.2÷1.4	3.0÷3.5	24	0.0223	33	0.0399	33	0.0695	34	0.0994	37	0.1229
7	1.6÷1.8	4.0÷4.5	6	0.0056	11	0.0132	8	0.0168	12	0.0351	11	0.0365
8	1.8÷2.0	4.5÷5.0	5	0.0047	10	0.0120	6	0.0126	5	0.0146	2	0.0066
9	2.0÷2.2	5.0÷5.5	2	0.0019	4	0.0048	4	0.0084	5	0.0146	2	0.0066
10	2.2÷2.4	5.5÷6.0	2	0.0019	1	0.0012	4	0.0084	2	0.0058	2	0.0066
11	2.4÷2.6	6.0÷6.5			0	0.0000	1	0.0021	1	0.0029		
12	2.6÷2.8	6.5÷7.0			2	0.0024			1	0.0029		
13	2.8÷3.0	7.0÷7.5			2	0.0024						
			1075		**836**		**442**		**342**		**301**	

n_i – number of interllamelar distances measured in the i-th class

n – number of measurements

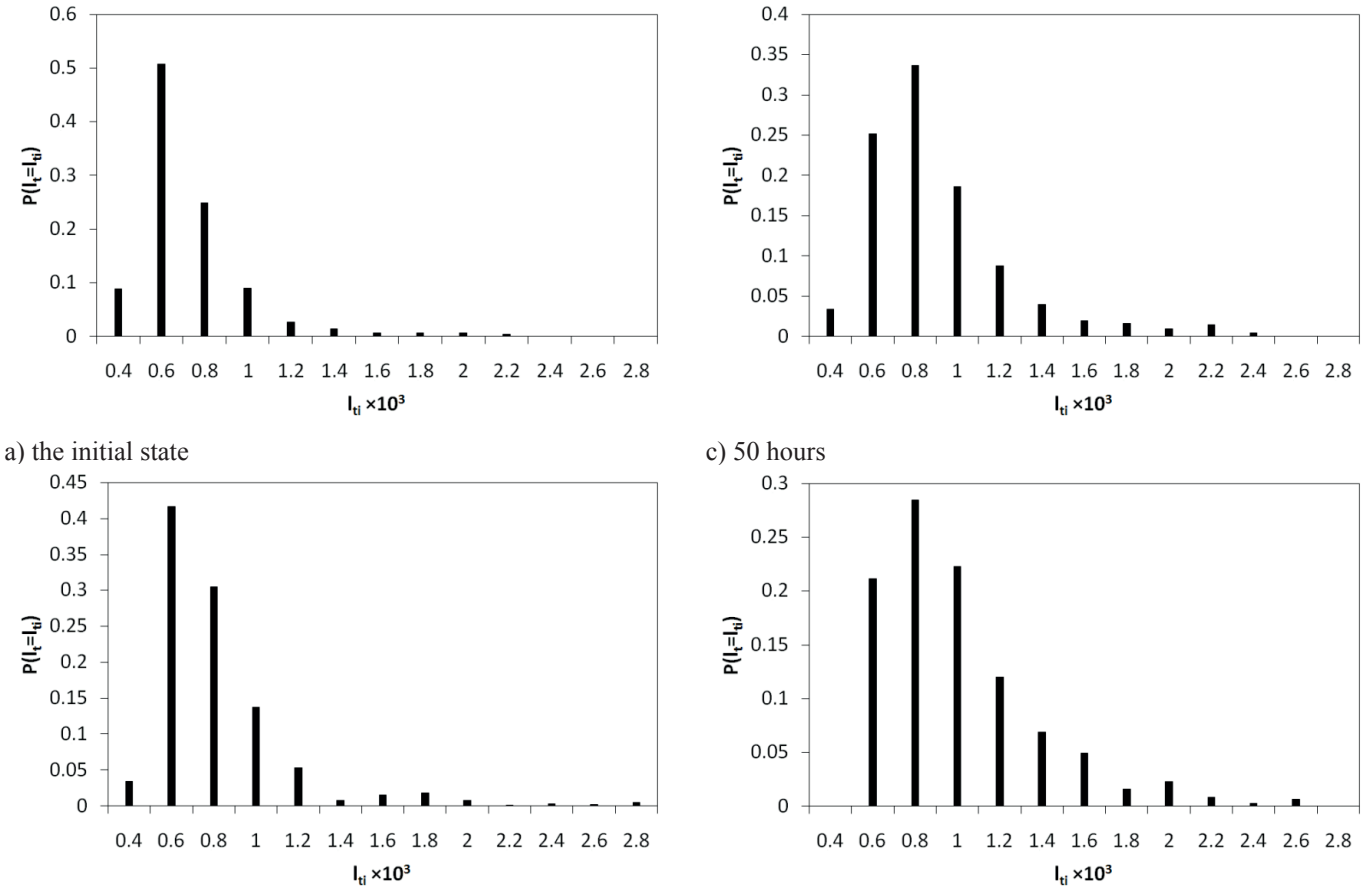

a) the initial state

c) 50 hours

b) 5 hours

d) 100 hours

Fig. 3. Distributions of the true interllamelar spacing after a) the initial state, b) 5, c) 50, d) 100

TABLE 2

Discrete distributions of the true interllamelar spacing

Class number	$l_{ti}/l_{a\,min}$	$l_{ti}\cdot10^3$, mm	$P(l_t = l_{ti})$				
			The initial state	5 hours	50 hours	100 hours	400 hours
1	1.0	0.4	0.089	0.034	0.034	-0.0130	-0.0047
2	1.5	0.6	0.508	0.417	0.252	0.2116	0.1366
3	2.0	0.8	0.249	0.305	0.337	0.2846	0.2555
4	2.5	1.0	0.090	0.137	0.186	0.223	0.2718
5	3.0	1.2	0.027	0.053	0.088	0.120	0.1449
6	3.5	1.4	0.014	0.008	0.040	0.069	0.1151
7	4.0	1.6	0.006	0.015	0.0195	0.049	0.0571
8	4.5	1.8	0.006	0.018	0.0157	0.016	0.0052
9	5.0	2.0	0.006	0.008	0.0095	0.0225	0.0052
10	5.5	2.2	0.004	0.001	0.014	0.0081	0.0134
11	6.0	2.4		0.003	0.0043	0.0023	
12	6.5	2.6		0.002		0.0062	
13	7.0	2.8		0.005			

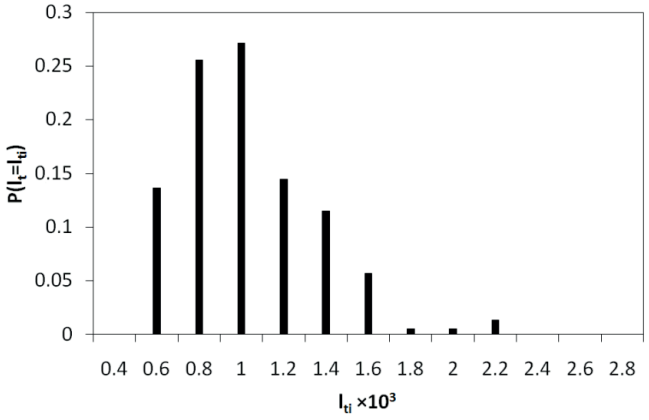

e) 400 hours

Fig. 3e. Distributions of the true interllamelar spacing after e) 400 hours

6. Summary

In the initial microstructure, i.e. after the pearlitic transformation, thick-lamellar pearlite is dominant. The non-lamellar fraction is small. In the course of the spheroidization process, the morphology of the microstructure changes in a typical manner; the fraction of the divorced pearlite increases gradually at the expense of the lamellar fraction. The spheroidization process runs non-uniformly. Even after longer annealing times, next to cementite particles, there are well-preserved areas of the lamellar structure. The longer the spheroidizing annealing time, the higher values of the distribution of the true interlamellar spacing, which points, in the statistical meaning, to a higher stability (durability) of the lamellar morphology in the case of a larger interlamellar spacing. The colonies of thick-lamellar pearlite are more stable. At the same time – as it was proven in earlier works [26, 27] – the crystallographic orientation of the phases in these colonies (Pitch, Bagariacki) is statistically similar to that in the initial pearlite. This suggests that, locally, the spheroidization ability is determined by the interlamellar spacing, and the general description of this ability should be based on the distribution of the interlamellar spacing.

Acknowledgements

The work has been implemented within framework of statutory research of AGH University of Science and Technology, contract No 11.11.110.299 AGH.

Received: 10 November 2015.

REFERENCES

[1] M. Hillert, The formation of pearlite, in: V.F. Zakay, H.I. Aaronson (Eds.), Decomposition of austenite by diffusional processes, New York, NY Interscience 1962.
[2] S.A. Hackney, G.J. Shiflet, Acta Metall. **35,** 1019-1028 (1987).
[3] S.N. Doi, H.J. Kestenbach, Metallography **23**, 135-146 (1989).
[4] T. Kozieł, P. Matusiewicz, M. Kopyściański, A. Zielińska-Lipiec, Metallurgy and Foundry Engineering **39**, 7-14 (2013).
[5] B. Pawłowski, P. Bała, J. Krawczyk, Metallurgy and Foundry Engineering **35**, 121-128 (2009).
[6] J.W. Martin, R.D. Doherty, Stability of Microstructure in Metallic Systems, Cambridge University Press 1976.
[7] M. McLean, Metal Science **3**, 113-122 (1978).
[8] F.A. Nichols, W.W. Mullins, Transactions of Metallurgical Society of AIME **233**, 1840-1848 (1965).
[9] Y.L. Tian, R.W. Kraft, Metallurgical Transaction A **18A**, 1403-1414 (1987).
[10] A.A. Baranow, Izwiestia Akademii Nauk SSSR. Metałły **3** 104-107 (1969).
[11] D. Goodchild, Scandinavian Journal of Metallurgical **1**, 235 – 240 (1972).
[12] W.W. Mullins, Journal of Applied Physics **28**, 333-339 (1957).
[13] G.H. Nijhof, Härterei Techn. Mitt. **35**, 59-68 (1980).
[14] G.H. Nijhof, Härterei Techn. Mitt. **36**, 242-247 (1981).
[15] Y.L. Tian, R.W. Kraft, Metallurgical Transaction A **18A**, 1359-1369 (1987)
[16] [T. Skowronek, A. Czarski, K. Satora, Materiały XXX Szkoły Inżynierii Materiałowej, Kraków Ustroń-Jaszowiec 205-209 (2002).
[17] R.T. DeHoff, F.N. Rhines, Quantitative Microscopy, New York, McGraw-Hill 1968.
[18] E.E. Underwood, Quantitative Stereology, Addison-Weseley 1970.
[19] A. Czarski, J. Ryś, Acta Stereologica **6**, 567-572 (1987).
[20] A. Czarski, P. Matusiewicz, Metallurgy and Foundry Engineering 41, (2015) (will be published).
[21] A. Czarski, E. Głowacz, Archives of Metallurgy and Materials 55, 101-105 (2010).
[22] J. Ryś, A. Czarski, Proc. of IV Symposium on Metallography, Vysoke Tatry, Czechoslovakia **1**, 25-30 (1986).
[23] A. Czarski, P. Matusiewicz, Metallurgy and Foundry Engineering **38**, 133-137 (2012).
[24] A. Czarski, J. Ryś, Pr. Kom. Metal.-Odlew., Pol. Akad. Nauk-Oddz. Krakow, Metalurgia **35**, 35-42 (1988).
[25] P. Matusiewicz, A. Czarski, H. Adrian, Metallurgy and Foundry Engineering **33**, 33-40 (2007).
[26] A. Czarski, T. Skowronek, W. Osuch, Metallurgy and Foundry Engineering, 33, 41-49 (2007).
[27] T. Skowronek, W. Ratuszek, K. Chruściel, A. Czarski, K. Satora, K. Wiencek, Archives of Metallurgy and Materials 49, 961-971 (2004)